Biochemistry

Communication

pubs.acs.org/biochemistry

Neutron and Atomic Resolution X-ray Structures of a Lytic Polysaccharide Monooxygenase Reveal Copper-Mediated Dioxygen Binding and Evidence for N-Terminal Deprotonation

John-Paul Bacik,[†,⊥] Sophanit Mekasha,[‡] Zarah Forsberg,[‡] Andrey Y. Kovalevsky,[§] Gustav Vaaje-Kolstad,[‡] Vincent G. H. Eijsink,[‡] Jay C. Nix,[∥] Leighton Coates,[§] Matthew J. Cuneo,[§] Clifford J. Unkefer,[†] and Julian C.-H. Chen[*,†]

[†]Protein Crystallography Station, Bioscience Division, Los Alamos National Laboratory, Los Alamos, New Mexico 87545, United States

[‡]Faculty of Chemistry, Biotechnology and Food Science, Norwegian University of Life Sciences (NMBU), PO Box 5003, 1430 Ås, Norway

[§]Biology and Soft Matter Division, Oak Ridge National Laboratory, 1 Bethel Valley Road, P.O. Box 2008, Oak Ridge, Tennessee 37831, United States

[∥]Advanced Light Source, Lawrence Berkeley Laboratory, 1 Cyclotron Road, Berkeley, California 94720, United States

Supporting Information

ABSTRACT: A 1.1 Å resolution, room-temperature X-ray structure and a 2.1 Å resolution neutron structure of a chitin-degrading lytic polysaccharide monooxygenase domain from the bacterium *Jonesia denitrificans* (*Jd*LPMO10A) show a putative dioxygen species equatorially bound to the active site copper. Both structures show an elongated density for the dioxygen, most consistent with a Cu(II)-bound peroxide. The coordination environment is consistent with Cu(II). In the neutron and X-ray structures, difference maps reveal the N-terminal amino group, involved in copper coordination, is present as a mixed ND_2 and ND^-, suggesting a role for the copper ion in shifting the pK_a of the amino terminus.

Lytic polysaccharide monooxygenases (LPMOs) are copper-dependent enzymes found in bacteria and fungi, utilizing an oxidative mechanism to cleave polysaccharides.[1,2] This family of enzymes has wide-ranging applications in biofuel production, as they are able to degrade a variety of polysaccharides, notably crystalline cellulose. The enzymes utilize a single copper ion to activate oxygen. While the catalytic mechanism of LPMOs remains uncertain, it is thought that catalysis involves initial formation of a superoxide by electron transfer from the reduced copper ion.[3−6] The copper ion is in a conserved histidine brace motif, using the side chain imidazole groups of two histidines, one of which is the N-terminal amino acid, along with the N-terminus itself, to coordinate the copper.[7] A number of X-ray crystallographic structures are currently available for LPMOs from fungal and bacterial species.[7−13] Identifying the oxidation state of the catalytic copper ion and copper-bound oxygen species, the protonation states of active site residues, and copper-bound ligands may offer potential clues about the enzyme's function.

Neutron diffraction has the ability to experimentally determine hydrogen atom positions, as the coherent scattering length of deuterium atoms, introduced into exchangeable moieties such as amides, amines, and hydroxyls, is 6.67 fm, comparable to those of other heavier elements in macromolecules like C, N, and O. This makes neutron diffraction a useful tool for determining protonation states and estimating pK_a values of critical catalytic residues, and for unambiguously orienting hydrogen bonding donor and acceptor pairs and solvent molecules.[14] Furthermore, radiation damage is negligible, allowing for data sets to be collected at more physiological temperatures.

To probe the protonation states of active site residues and species bound to the copper, neutron diffraction data were collected to 2.1 Å resolution on a large crystal of a chitin-degrading LPMO domain from the Gram-positive bacterium *Jonesia denitrificans* (*Jd*LPMO10A), which uses an oxidative mechanism to cleave at the C1 position in the scissile glycosidic bond.[15] Labile hydrogen atoms in the crystal were exchanged using D_2O-containing mother liquor, to make them visible in nuclear density maps as deuteriums. The model was refined to R_{free} and R_{cryst} values of 26.5 and 18.7%, respectively, using the program Phenix (Table S1). The crystal used for the experiment was not exposed to X-rays, avoiding potential structural changes due to X-ray-induced photoreduction, the occurrence of which has been well-documented by other groups that have studied copper proteins.[9,10] Using a separate crystal grown under identical crystallization conditions, room-temperature X-ray diffraction data to 1.1 Å were collected at beamline 4.2.2 at the Advanced Light Source, with careful efforts to minimize radiation damage and the potential for photoreduction, as described previously.[15] The X-ray structure of *Jd*LPMO10A was determined and refined to R_{free} and R_{cryst} values of 12.8 and 11.4%, respectively (Table S1), extending the resolution of our previous 1.55 Å structure collected at 100 K.[8]

Received: January 10, 2017
Revised: May 3, 2017
Published: May 8, 2017

DOI: 10.1021/acs.biochem.7b00019
Biochemistry 2017, 56, 2529−2532

Together, these data provide insights regarding the oxidation state of the catalytic copper ion, potential oxygen species bound to the enzyme, and the protonation state of residues near the copper site.

The protein crystallizes with two molecules occupying distinct microenvironments in the asymmetric unit. In the active site of the X-ray structure (Figure 1), the catalytic copper ion is coordinated by a so-called histidine brace found in all LPMOs that utilize the side chains of two conserved histidine residues, the N-terminal residue His32 and His109, and the N-terminal amino group of His32 (residues 1−31 comprise the signal sequence).[7−9,11,13,16] As shown in panels C and D of Figure 1, the copper coordination environments in the two monomers are similar, though not identical. The three nitrogen atoms form an equatorial plane. The final equatorial site in the X-ray structure is modeled as a dioxygen species, as confirmed by omit maps depicting strong $F_o - F_c$ difference density when one of the oxygens is omitted from the dioxygen (Figure S1). The two molecules exhibit slightly different modes of oxygen binding. In molecule A, the dioxygen appears to be in a bidentate coordination environment, while in molecule B, the dioxygen is coordinated end-on (Table S2). The distal axial coordination site is occupied by water. Access to the proximal axial site is restricted by Phe164, as is commonly observed in LPMOs, which carry a Phe or a Tyr at this position.

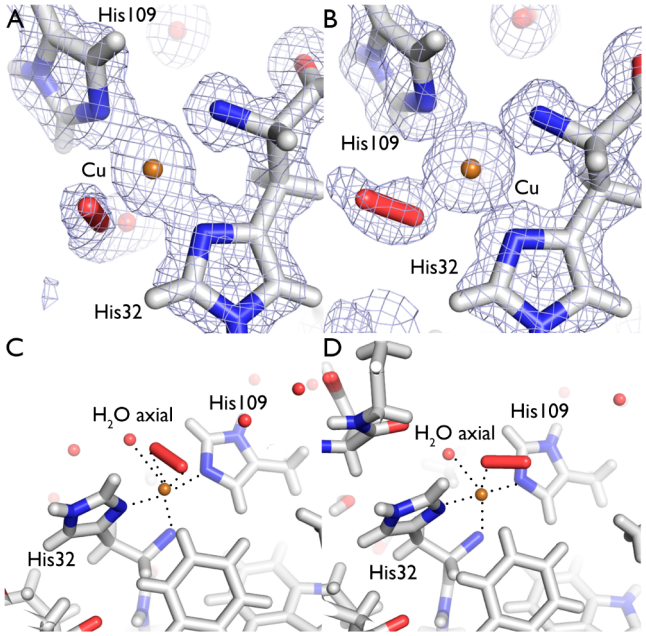

Figure 1. $2F_o - F_c$ electron density (lavender) for (A) molecule A and (B) molecule B of the 1.1 Å room-temperature X-ray structure, contoured at 1.0σ, showing the active site coordination environment. The oxygen species coordinated to the copper ion has been modeled as peroxide with an O−O bond length of 1.5 Å. Active site copper coordination environment for (C) molecule A and (D) molecule B. Coordination distances are detailed in Table S2.

In the X-ray crystallographic structure, the refined coordination distances between the copper ion and the nitrogen ligands average to 2.0−2.2 Å (Figure 1C,D and Table S2). The square bipyramidal geometry and the presence of water/oxygen ligands suggest a Cu(II) oxidation state, consistent with other crystal structures of LPMO enzymes reported in the literature.[9,10,17] In an EXAFS and XANES study of a tetrapeptide−copper complex, the Cu(II)−nitrogen distance is 1.9 Å and the Cu(III)−nitrogen distance is slightly shorter, 1.8 Å.[18] The coordination distances seen in the X-ray crystallographic structure do not support a Cu(III) state. The geometry of the coordination is also distinct from the T-shaped coordination seen in Cu(I) complexes.

PROTONATION STATES IN THE ACTIVE SITE

The protonation states of active site residues were examined in the nuclear density maps. Nuclear density for the copper ion is weak, as has been observed for metals in other metalloenzymes such as carbonic anhydrase, xylose isomerase, and DFPase.[19−21] Of particular interest is the protonation state of the amino terminus. The amino terminus in molecule A is observed as ND_2 based on a difference $F_o - F_c$ map calculated without the deuterium atoms, which shows a planar difference peak for the two deuteriums. Notably though, the N-terminus in molecule B shows an asymmetric $F_o - F_c$ difference peak in the nuclear density maps, suggesting the presence of a mixed ND_2 and ND^- species (Figure 2). This was further confirmed using nuclear $F_o - F_c$ omit maps (Figure S2).

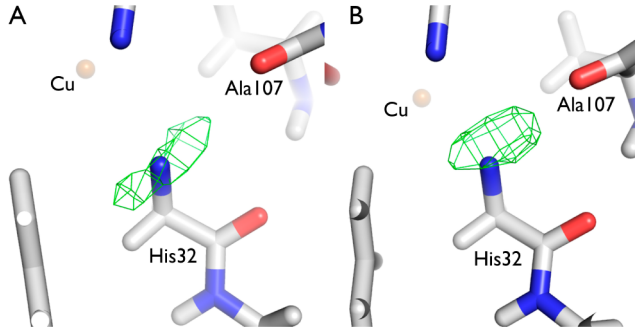

Figure 2. Active site of the two LPMO molecules in the asymmetric unit, showing $F_o - F_c$ nuclear difference density (green) contoured at 3.0σ corresponding to (A) a ND_2 in molecule A and (B) a putative ND^- species in molecule B, with the deuterium pointing toward the carbonyl of Ala107.

To further examine this observation, the electron density around the amino terminus was re-examined in the room-temperature X-ray structure. The very high resolution (1.1 Å) is such that the $F_o - F_c$ difference density for a limited number of hydrogen (or deuterium) atoms can be discerned. Although no difference density was seen in molecule A, on the basis of these difference maps, the protonation state of the N-terminal amino group in molecule B appears to be also a mixed ND_2 and ND^-, similar to the neutron structure (Figure S3A). *Jd*LPMO10A was crystallized at pH 7.0, and given the observation of mixed ND^- and ND_2 species, the pK_a of the amino terminus is estimated to be approximately 7−7.5. Of note are electron density maps in the high resolution (1.37 Å) structure of *Neurospora crassa* LPMO9M (Protein Data Bank entry 4EIS),[22] crystallized at pH 8.5, which have the N-terminus modeled as a NH_2. One of the hydrogen atoms has a negative $F_o - F_c$ peak, indicating the presence of an NH^- group (Figure S3B). It is likely that a similar protonation state for the N-terminus may be found in other members of the LPMO family, and this may be of significance to the reaction mechanism.

DOI: 10.1021/acs.biochem.7b00019
Biochemistry 2017, 56, 2529−2532

OXYGEN SPECIES

In the neutron structure, one of the two molecules in the asymmetric unit shows what appears to be a dioxygen species. The density strongly suggests that the copper ion in molecule B coordinates a dioxygen species, although the resolution of the structure does not easily permit its unambiguous identification (Figure 3). The density appears to be too long for an O═O

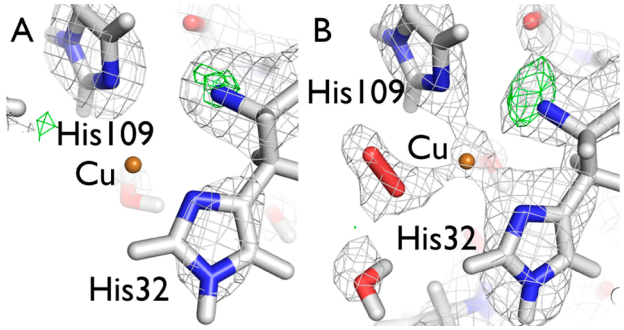

Figure 3. $2F_o - F_c$ composite omit nuclear density in the active site region (gray), contoured at 1.5σ, for (A) molecule A and (B) molecule B. $F_o - F_c$ difference density (green), contoured at 3.0σ, is overlaid. No difference density is seen around the oxygen species that is present in molecule B.

(1.21 Å) or superoxo (1.33 Å) species and is most consistent with the bond length of a peroxide (1.49 Å). Nevertheless, the bond length of the dioxygen species may be influenced by binding to copper. The shape of the $2F_o - F_c$ density and the lack of $F_o - F_c$ density in the vicinity of the dioxygen suggest that the dioxygen species is not protonated, which likely excludes hydrogen peroxide (as DO−OD) or hydroperoxo (as $^{-}$O−OD) as the bound species, as the D scatters neutrons strongly. Still, we cannot rule out flexibility in binding of the dioxygen species, which could obscure the strong scattering contribution from a bound deuterium. Interestingly, putative oxygen species have been observed previously in LPMOs at axial positions and farther from the copper.[22,23] Here, we show crystallographic evidence of a dioxygen species in an equatorial position that is clearly interacting with the copper. The position of this species is compatible with the recently determined X-ray structure of an LPMO in complex with a cello-oligosaccharide and the mechanistic inferences made from the structure, as well as recent crystallographic data regarding an LPMO from *N. crassa*, discussed in more detail below.[11,23]

FUNCTIONAL IMPLICATIONS

The bracing N-terminal group contains mixed ND_2 and ND^- as observed in both the X-ray and neutron structures. The pK_a values for copper-coordinated amines in model Cu(III) complexes have been reported to range from 8 to 10.[24] We have not found reports for pK_a's of Cu(II)-coordinated amines. The pK_a values for Cu(II)-coordinated amides have been reported to be between 7.8 and 8.8, illustrating that coordination of nitrogen by copper can significantly lower the pK_a, in the case of amides, to near-physiological pH values.[25] Given that the protein was crystallized at pH 7.0, well within the pH range of enzymatic activity for bacterial LPMOs (e.g., refs 1, 26, and 27), the pK_a for deprotonation of the bracing amine ($-NH_2$), may be in the neutral pH range. As noted by Quinlan et al.[7] and Walton and Davies,[3] a deprotonated amino terminus could stabilize a potential Cu(III)−OH intermediate. The observation of mixed ND_2 and ND^- in the two molecules in the crystal asymmetric unit is plausible, given their different crystal packing environments.

A set of ultra-high resolution X-ray and neutron structures of *Nc*LPMO9D, an LPMO from the fungus *N. crassa* (also known as NCU01050 and PMO-2), crystallized at pH 5.6, was recently reported.[23] While *Nc*LPMO9D and *Jd*LPMO10A share a similar β-sandwich inner core fold and active site environment, they exhibit low levels of sequence (~10% identical) and structural similarity and have different preferred substrates.[17] *Jd*LPMO10A cleaves glycosidic bonds by oxidizing C1 of the β1−4 linkage in chitin, while *Nc*LPMO9D oxidizes C4 of the β1−4 linkage in cellulose. *Nc*LPMO9D contains an axial tyrosine that coordinates the catalytic copper, albeit with an elongated Cu−O separation, while in *Jd*LPMO10A, the tyrosine position is occupied by a phenylalanine that does not coordinate the copper. From the neutron structure of *Nc*LPMO9D, it was suggested that a neutral or protonated histidine residue (His157) in the vicinity of the active site, distinct from the histidine residues coordinating the catalytic copper, may be critical in the reaction mechanism by interacting with and preorganizing O_2 prior to it entering the copper center. Notably, there is no analogous residue in *Jd*LPMO10A or other chitin-active LPMO10s,[16] whereas a similar histidine occurs in some, but far from all, cellulose-active LPMO10s. Still, most importantly, the X-ray structural studies of ascorbate-treated *Nc*LPMO9D crystals revealed an equatorially bound dioxygen in one of the molecules in the asymmetric unit, which was modeled as a peroxo species directly coordinating the catalytic copper ion, adopting a similar end-on binding configuration (Table S2).[23]

While many of the details of the LPMO mechanism remain to be resolved, the data presented here and in other recent studies[11,23] strongly indicate that catalysis involves equatorial binding of a reactive oxygen species, as anticipated by Kjærgaard et al.[4] Importantly, while LPMOs show large sequence variation and even display considerable differences in the axial copper coordination positions,[9,17,28] this study of a bacterial LPMO and other recent studies that include fungal LPMOs suggest a high degree of mechanistic similarity.

ASSOCIATED CONTENT

Supporting Information

The Supporting Information is available free of charge on the ACS Publications website at DOI: 10.1021/acs.biochem.7b00019.

Materials and Methods, Tables S1 and S2, and Figures S1−S3 (PDF)

AUTHOR INFORMATION

Corresponding Author

*E-mail: chen_j@lanl.gov. Phone: +1.505.664.0181.

ORCID

Andrey Y. Kovalevsky: 0000-0003-4459-9142

Julian C.-H. Chen: 0000-0003-0341-165X

Present Address

⊥J.-P.B.: Department of Chemistry, Princeton University, Princeton, NJ 08544.

Funding

This work was supported by The Research Council of Norway through Grants 214613, 221576, and 249865 and by the Vista

DOI: 10.1021/acs.biochem.7b00019
Biochemistry 2017, 56, 2529−2532

program of the Norwegian Academy of Science and Letters (Grant 6510). J.-P.B., J.C.-H.C., and C.J.U. were funded by the Department of Energy Office of Biological and Environmental Research.

Notes

The authors declare no competing financial interest.

■ ACKNOWLEDGMENTS

We thank Dr. William Woodruff for helpful discussions and insights. The MaNDi instrument at the Spallation Neutron Source was sponsored by the Scientific User Facilities Division, Office of Basic Energy Sciences, of the Department of Energy. The Advanced Light Source is supported by the Director, Office of Science, Office of Basic Energy Sciences, of the U.S. Department of Energy under Contract DE-AC02−05CH11231.

■ REFERENCES

(1) Vaaje-Kolstad, G., Westereng, B., Horn, S. J., Liu, Z., Zhai, H., Sorlie, M., and Eijsink, V. G. H. (2010) *Science 330*, 219−222.
(2) Horn, S. J., Vaaje-Kolstad, G., Westereng, B., and Eijsink, V. G. H. (2012) *Biotechnol. Biofuels 5*, 45.
(3) Walton, P. H., and Davies, G. J. (2016) *Curr. Opin. Chem. Biol. 31*, 195−207.
(4) Kjaergaard, C. H., Qayyum, M. F., Wong, S. D., Xu, F., Hemsworth, G. R., Walton, D. J., Young, N. A., Davies, G. J., Walton, P. H., Johansen, K. S., Hodgson, K. O., Hedman, B., and Solomon, E. I. (2014) *Proc. Natl. Acad. Sci. U. S. A. 111*, 8797−8802.
(5) Kim, S., Ståhlberg, J., Sandgren, M., Paton, R. S., and Beckham, G. T. (2014) *Proc. Natl. Acad. Sci. U. S. A. 111*, 149−154.
(6) Beeson, W. T., Vu, V. V., Span, E. A., Phillips, C. M., and Marletta, M. A. (2015) *Annu. Rev. Biochem. 84*, 923−946.
(7) Quinlan, R. J., Sweeney, M. D., Lo Leggio, L., Otten, H., Poulsen, J.-C. N., Johansen, K. S., Krogh, K. B. R. M., Jørgensen, C. I., Tovborg, M., Anthonsen, A., Tryfona, T., Walter, C. P., Dupree, P., Xu, F., Davies, G. J., and Walton, P. H. (2011) *Proc. Natl. Acad. Sci. U. S. A. 108*, 15079−15084.
(8) Mekasha, S., Forsberg, Z., Dalhus, B., Bacik, J.-P., Choudhary, S., Schmidt-Dannert, C., Vaaje-Kolstad, G., and Eijsink, V. G. H. (2016) *FEBS Lett. 590*, 34−42.
(9) Hemsworth, G. R., Taylor, E. J., Kim, R. Q., Gregory, R. C., Lewis, S. J., Turkenburg, J. P., Parkin, A., Davies, G. J., and Walton, P. H. (2013) *J. Am. Chem. Soc. 135*, 6069−6077.
(10) Gudmundsson, M., Kim, S., Wu, M., Ishida, T., Momeni, M. H., Vaaje-Kolstad, G., Lundberg, D., Royant, A., Stahlberg, J., Eijsink, V. G. H., Beckham, G. T., and Sandgren, M. (2014) *J. Biol. Chem. 289*, 18782−18792.
(11) Frandsen, K. E. H., Simmons, T. J., Dupree, P., Poulsen, J. C. N., Hemsworth, G. R., Ciano, L., Johnston, E. M., Tovborg, M., Johansen, K. S., von Freiesleben, P., Marmuse, L., Fort, S., Cottaz, S., Driguez, H., Henrissat, B., Lenfant, N., Tuna, F., Baldansuren, A., Davies, G. J., Lo Leggio, L., and Walton, P. H. (2016) *Nat. Chem. Biol. 12*, 298−303.
(12) Forsberg, Z., MacKenzie, A. K., Soerlie, M., Roehr, A. K., Helland, R., Arvai, A. S., Vaaje-Kolstad, G., and Eijsink, V. G. H. (2014) *Proc. Natl. Acad. Sci. U. S. A. 111*, 8446−8451.
(13) Chaplin, A. K., Wilson, M. T., Hough, M. A., Svistunenko, D. A., Hemsworth, G. R., Walton, P. H., Vijgenboom, E., and Worrall, J. A. R. (2016) *J. Biol. Chem. 291*, 12838−12850.
(14) Chen, J. C.-H., Hanson, B. L., Fisher, S. Z., Langan, P., and Kovalevsky, A. Y. (2012) *Proc. Natl. Acad. Sci. U. S. A. 109*, 15301−15306.
(15) Bacik, J.-P., Mekasha, S., Forsberg, Z., Kovalevsky, A., Nix, J. C., Cuneo, M. J., Coates, L., Vaaje-Kolstad, G., Chen, J. C.-H., Eijsink, V. G. H., and Unkefer, C. J. (2015) *Acta Crystallogr., Sect. F: Struct. Biol. Commun. 71*, 1448−1452.
(16) Forsberg, Z., Roehr, A. K., Mekasha, S., Andersson, K. K., Eijsink, V. G. H., Vaaje-Kolstad, G., and Soerlie, M. (2014) *Biochemistry 53*, 1647−1656.
(17) Vaaje-Kolstad, G., Forsberg, Z., Loose, J. S. M., Bissaro, B., and Eijsink, V. G. H. (2017) *Curr. Opin. Struct. Biol. 44*, 67−76.
(18) Pratesi, A., Giuli, G., Cicconi, M. R., Della Longa, S., Weng, T. C., and Ginanneschi, M. (2012) *Inorg. Chem. 51*, 7969−7976.
(19) Blum, M.-M., Mustyakimov, M., Rüterjans, H., Kehe, K., Schoenborn, B. P., Langan, P., and Chen, J. C.-H. (2009) *Proc. Natl. Acad. Sci. U. S. A. 106*, 713−718.
(20) Fisher, S. Z., Kovalevsky, A. Y., Domsic, J. F., Mustyakimov, M., McKenna, R., Silverman, D. N., and Langan, P. A. (2010) *Biochemistry 49*, 415−421.
(21) Kovalevsky, A., Hanson, B. L., Mason, S. A., Forsyth, V. T., Fisher, Z., Mustyakimov, M., Blakeley, M. P., Keen, D. A., and Langan, P. (2012) *Acta Crystallogr., Sect. D: Biol. Crystallogr. 68*, 1201−1206.
(22) Li, X., Beeson, W. T., Phillips, C. M., Marletta, M. A., and Cate, J. H. D. (2012) *Structure 20*, 1051−1061.
(23) O'Dell, W. B., Agarwal, P. K., and Meilleur, F. (2017) *Angew. Chem., Int. Ed. 56*, 767−770.
(24) McDonald, M. R., Fredericks, F. C., and Margerum, D. W. (1997) *Inorg. Chem. 36*, 3119−3124.
(25) Kroneck, P. M. H., Vortisch, V., and Hemmerich, P. (1980) *Eur. J. Biochem. 109*, 603−612.
(26) Vaaje-Kolstad, G., Boehle, L. A., Gåseidnes, S., Dalhus, B., Bjørås, M., Mathiesen, G., and Eijsink, V. G. H. (2012) *J. Mol. Biol. 416*, 239−254.
(27) Forsberg, Z., Nelson, C. E., Dalhus, B., Mekasha, S., Loose, J. S. M., Crouch, L. I., Roehr, A. K., Gardner, J. G., Eijsink, V. G. H., and Vaaje-Kolstad, G. (2016) *J. Biol. Chem. 291*, 7300−7312.
(28) Borisova, A. S., Isaksen, T., Dimarogona, M., Kognole, A. A., Mathiesen, G., Várnai, A., Røhr, Å. K., Payne, C. M., Sørlie, M., Sandgren, M., and Eijsink, V. G. H. (2015) *J. Biol. Chem. 290*, 22955−22969.

DOI: 10.1021/acs.biochem.7b00019
Biochemistry 2017, 56, 2529−2532